

Elastic Precursor Decay and Spallation in Nonporous Tungsten Carbide Ceramics

A. S. Savinykh^{a,*}, I. A. Cherepanov^{a,b}, S. V. Razorenov^a, K. Mandel^c, and L. Krüger^c

^a Institute of Problems of Chemical Physics, Russian Academy of Sciences,
Chernogolovka, Moscow oblast, 142432 Russia

^b Moscow State University, Moscow, 119991 Russia

^c Freiberg University of Mining and Technology, Freiberg, 09599 Germany

*e-mail: savas@fcp.ac.ru

Received July 4, 2018

Abstract—To identify the possible contribution of relaxation processes to the resistance against high-rate deformation, evolution of shock-compression waves in tungsten carbide (WC) ceramics manufactured by spark-plasma sintering at a maximum compressive stress of 27 GPa is measured. Strong elastic precursor decay upon changing the thickness of the samples from 0.15 to 4 mm is revealed. At maximum shock compressive stresses twice exceeding the Hugoniot elastic limit, a decrease in the spall strength value by about 30% from its value in the elastic region is recorded.

DOI: 10.1134/S1063784219030216

INTRODUCTION

Along with broad applications in different industries, superhard ceramics are often used under conditions of intense shock loads. Due to the high cost of complex ceramic products, forecasting the results of shock impacts by computer simulation becomes a topical problem. To build adequate models and determine relations describing the resistance to high-rate deformation and fracture under conditions of high-velocity impact, it is important to correctly assess, in particular, the contribution of the relaxation of stresses in this time interval.

Review [1] summarizes the data on Hugoniot elastic limit decay in superhard brittle materials. According to this paper, decay of the elastic precursor wave with relaxation of stresses behind its front is recorded in plane-wave experiments with boron carbide ceramics, insignificant decay is observed in dolomite, and dense limestone shows slight decay or its absence. Insignificant elastic precursor decay is also observed in experiments with quartzite [2] and alumina ceramics [3]. In [4], the absence of dependence of the Hugoniot elastic limit of alumina ceramics on sample thickness is shown.

Experiments with S200F hot-pressed beryllium [5] showed monotonic decay of its Hugoniot elastic limit from 0.14 to 0.08 GPa in the samples with a thickness from 4 to 8 mm. In recent study [6], elastic precursor decay in alumina ceramics was recorded and it was found that a decrease in thickness from 3 to 0.25 mm gives rise to an increase in the Hugoniot elastic limit

value from 6.5 to 13 GPa at room temperature of the samples. The formation of a spike in alumina ceramics begins at the initial temperatures exceeding 800 K in samples with a thickness of less than 3 mm.

In [7], experiments on shockwave loading of alumina ceramics synthesized by spark-plasma sintering were conducted. It is shown that the Hugoniot elastic limit of investigated ceramics, which was measured for specimens with a thickness from 0.28 to 6 mm, decreases from 21 to 12 GPa, respectively. The spall strength of specimens with a thickness of 3 mm monotonically decreases from about 1.5 to about 0.3 GPa when increasing the maximum compressive stress to 29 GPa, which more than twice exceeds the Hugoniot elastic limit. Experiments with reaction-sintered silicon carbide ceramics with a thickness from 0.5 to 8.3 mm, the results of which are published in [8], do not observe elastic precursor decay and show that the evolution of the compression wave corresponds to a simple wave. It should be noted that the specimens studied were carved by the electro-erosion method practically without any impact on their internal structure.

In this paper, we study the evolution of a compression wave during its propagation in nonporous tungsten carbide ceramics. Such measurements for metals and alloys usually show the decay of elastic precursors of shock waves, an analysis of which gives information about the initial speed of the relaxation of stresses and the corresponding velocity of plastic deformation.

Table 1. Mechanical properties of investigated WC ceramics

ρ_0 , g/cm ³	ρ_{rel} , %	c_s , m/s	c_l , m/s	ν	E , GPa	G , GPa	d_{WC} , nm	HV 10	K_{Ic} , MPa m ^{1/2}
15.66	99.9	4384	7164	0.201	723	301	330	2690	6.7

ρ_0 is the density of samples; ρ_{rel} is the ratio of the measured density to theoretical density; c_s is the shear speed of sound; c_l is the longitudinal velocity of sound; ν is Poisson's ratio; E and G are Young's modulus and the shear modulus, respectively; d_{WC} is the mean grain size; HV 10 is the Vickers hardness; and K_{Ic} is the critical coefficient of the intensity of stresses.

EXPERIMENTAL

Nonporous samples of tungsten carbide ceramics were synthesized by sintering the powder of DN-4 pure tungsten carbide (H.C. Starck, Germany) by the plasma-spark method (spark plasma sintering (SPS) [9]) at a temperature of 1800°C for 3 min. Compared to traditional methods, SPS allows one to prepare high-quality sintered materials at lower temperatures and in shorter time. In Table 1, the mechanical properties of the studied ceramics are given. The methods for determining the mechanical properties of the studied tungsten carbide ceramics are described in detail in [10].

The initial samples of tungsten carbide represented plane-parallel plates with a thickness of 4 mm and a diameter of 20 mm. Samples with a nominal thickness of 2, 1, 0.5, 0.3, and 0.15 mm for shock-wave experiments were carved from the same initial plate by the electro-erosion method and were then polished. Experimental data for specimens with a thickness of 4 mm are taken from [10]. Samples with a thickness of 4 mm, which have been studied in [10], and samples, from which plates with a smaller thickness were carved, were synthesized at the same time and under the same conditions. The mechanical properties of fabricated specimens with a thickness of 4 mm do not change from sample to sample within measurement errors. The transverse dimensions of investigated specimens were sufficient to ensure conditions for one-dimensional deformation during the entire recording time.

The loading of the samples in the experiments on determining the Hugoniot elastic limit were carried out by the impact of an aluminum plate with a thickness of 2 mm at a speed of 1.8 ± 0.05 km/s through an aluminum screen with a thickness of 2 mm, which corresponds to a maximum shock compressive stress of about 27 GPa. The base plate was used for cutting off the air wave formed before a flying impactor. Throwing of impactors was carried out using explosive devices [11]. For determining critical tensile stresses, the samples were loaded by the impact of an aluminum plate with a thickness 0.38 mm at velocities of 0.62 ± 0.03 and 1.2 ± 0.03 km/s and an aluminum plate with a thickness of 2 mm at a velocity of 1.8 ± 0.05 km/s. During the loading of samples, free-surface velocity profiles $u_s(t)$ were recorded using a VISAR

laser Doppler velocimeter [12] with a time resolution of about 1 ns.

RESULTS AND DISCUSSION

Free-surface velocity profiles of tungsten carbide samples with a nominal thickness from 0.15 to 4 mm are shown in Fig. 1, which are measured under the conditions of the impact of an aluminum plate with a thickness of 2 mm at a speed of 1.8 km/s. The emergence of an elastic compression shock wave on the surface is recorded in the wave profiles, which is accompanied by the formation of a so-called "spike," i.e., a descending profile associated with intensive multiplication of dislocation-type defects and liberation of a plastic front. After that, a plastic compression wave reaches the surface. As can be seen from Fig. 1, recorded maximum velocity u_{HEL} of the free surface in the front of the elastic wave increases with a decrease in the sample thickness. Relaxation of stresses behind the elastic precursor wave front is not recorded in all experiments; the relaxation effect was most clearly observed in specimens with a thickness of 0.5 mm or less. The recorded profiles show good reproducibility from experiment to experiment and are characterized by the absence of oscillations, which indicates homogeneity of deformation in the plastic flow region.

A second rise of the velocity is recorded in wave profiles for samples with a thickness of less than 2 mm, which is caused by repeated reflection of a rarefaction wave from the base plate—sample surface. Since the dynamic impedance of WC ceramics is higher than the dynamic impedance of an aluminum base plate, the reflection of a rarefaction wave is accompanied by changing its sign and the repeatedly reflected wave becomes a compression wave as a result. In Lagrangian coordinates, the mean velocities of the fronts of rarefaction waves propagating in compressed material and compression waves propagating in unloaded material are in the range of 7.56 ± 0.1 km/s, which is slightly higher than the longitudinal velocity of sound at zero pressure. This indirectly indicates that the material has not been fractured during processes of one-dimensional compression and subsequent unloading, since the presence of cracks and other deformation defects has a significant effect on the velocity of propagation of perturbations.

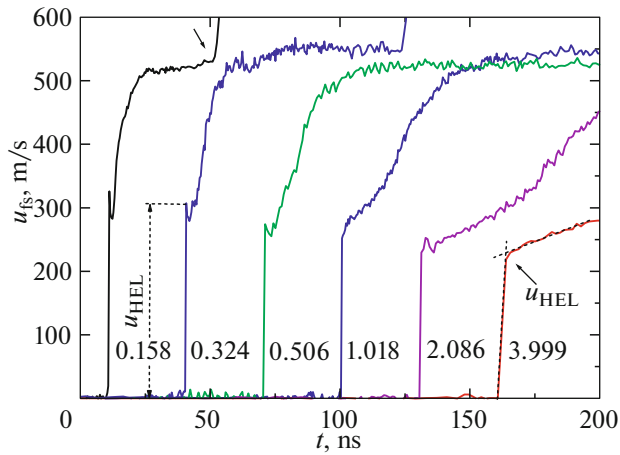


Fig. 1. Free-surface velocity profiles of samples of tungsten carbide ceramics with a thickness from 0.15 to 4 mm measured under the conditions of impact of an aluminum plate with a thickness of 2 mm at a velocity of 1.8 km/s. Numbers indicate the thicknesses of samples in millimeters, and the arrow at the velocity profile of the sample with a thickness of 0.158 mm points to the emergence of a repeatedly reflected compression wave on the surface.

The value of Hugoniot elastic limit σ_{HEL} was evaluated from the measured free-surface velocity profile as $\sigma_{\text{HEL}} = \rho_0 c u_{\text{HEL}}/2$ [11], where u_{HEL} is the maximum value of the free-surface velocity in the front of the elastic compression wave (Fig. 1). The results are given in Table 2. The results of processing wave profiles shown in Fig. 1 are given in Fig. 2 in the form of a dependence of the Hugoniot elastic limit on the thickness of a specimen in logarithmic coordinates. As can be seen from Fig. 2, the value of the Hugoniot elastic limit of tungsten carbide ceramics exponentially decreases with an increase in the distance traveled by an elastic wave. Moreover, a small spread in the data is observed in all cases under the same experimental conditions. The obtained data on elastic precursor decay given in Fig. 2 can be described with satisfactory accuracy by power relation $\sigma_{\text{HEL}} = S(h/h_0)^{-\alpha}$, where $h_0 = 1$ mm, $S = 14.72$ GPa, and $\alpha = 0.107$.

In Fig. 2, the obtained values of the Hugoniot elastic limit for WC ceramics are also compared with published data. In [13], the behavior of hot-pressed tungsten carbide ceramics is studied under conditions of shock compression. The measured Hugoniot elastic limit for samples with a thickness from 3 to 6 mm was 6.6 ± 0.5 GPa. Samples with a thickness of 4 mm synthesized by SPS exhibit a two-fold increase in the elastic compressive stress in comparison with hot-pressed samples, which can be explained by lower porosity of the former. The introduction of additives to tungsten carbide ceramics reduces its σ_{HEL} by more than two times for ceramics obtained by SPS [10] and almost three times for hot-pressed ceramics [14].

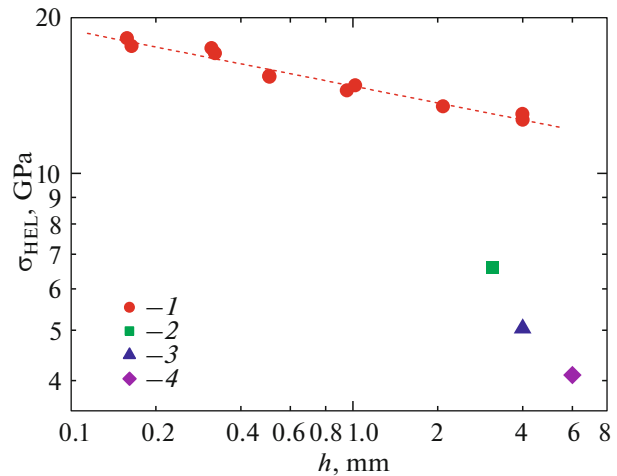


Fig. 2. Dependence of the Hugoniot elastic limit of WC ceramics on the sample thickness: (1) data obtained in this study; (2) data for hot-pressed WC Sercom [13]; (3) data for WC + Co (6%) synthesized by the SPS method [10]; (4) data for WC + Co (5.7%) + Ta (1.9%) [14].

The free-surface velocity profiles of a tungsten carbide sample with a nominal thickness of 4 mm [10] under conditions of impact of an aluminum plate with a thickness of 2 mm at a velocity of 1.8 km/s and a tungsten carbide sample with a nominal thickness of 1 mm under conditions of impact of an aluminum plate with a thickness of 0.38 mm at velocities of 1.2 and 0.62 km/s are shown in Fig. 3. The ratio of the thicknesses of the sample and impactor in these experiments is adjusted in such a way that conditions for spallation of the specimen could be created and thus its spall strength could be determined. The wave profiles given in Fig. 3 show all peculiarities of the fracture of an elastic plastic material under conditions of spallation, such as: the emergence of an elastic-plastic compression wave on the sample surface; a rarefaction wave following it; the point in time when spallation starts, which coincides with the first minimum of the

Table 2. Results of the experiments on measuring the Hugoniot elastic limit with tungsten carbide samples

h , mm	u_{HEL} , m/s	σ_{HEL} , GPa
0.158	325	18.18
0.164	314	17.57
0.315	311	17.41
0.324	304	17.01
0.506	274	15.34
0.505	275	15.39
1.018	264	14.77
2.086	240	13.46
3.995 [10]	232	13.01
3.999 [10]	227	12.68

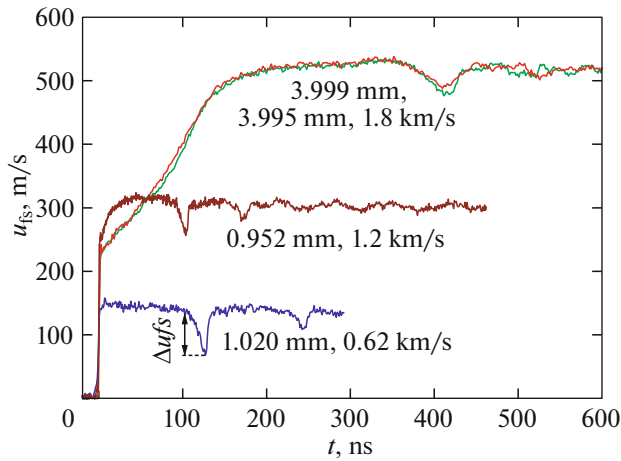


Fig. 3. Free-surface velocity profiles of samples of tungsten carbide ceramics measured under the conditions of the impact of an aluminum plate at velocities of 1.8 [10], 1.2, and 0.62 km/s. Numbers indicate the thicknesses of samples and the speed of the aluminum impactor at the time of its collision with the sample.

velocity in the wave profile; the formation of a compression pulse or so-called “spallation pulse”; and subsequent fluctuations in the speed of the surface associated with its reverberation in the spallation plate. In the experiment with loading created by an impactor accelerated to 0.62 km/s, the created maximum compression pressure is lower than the Hugoniot elastic limit, i.e., the spallation of the sample occurs in the elastic region.

The spall strength was calculated from measured value Δu_{fs} of a velocity drop in the rarefaction wave before the front of the spallation pulse (Fig. 3) by the following formula [11]: $\sigma_{sp} = \rho_0 c_l \Delta u_{fs} / 2$. The obtained values of spall strength at an estimated deformation rate of about $3 \times 10^5 \text{ s}^{-1}$ in the rarefaction wave are given in Table 3.

The dependence of spall strength on the maximum stress of tungsten carbide ceramics in comparison with published data is given in Fig. 4. To calculate the ratio of maximum stress to the Hugoniot elastic limit, the measured σ_{HEL} value corresponding to sample thickness was used. It is clearly visible that the largest value of spall strength is implemented in the elastic region.

Table 3. Results of the experiments on measuring spall strength with tungsten carbide samples

h , mm	Δu_{fs} , m/s	σ_{max} , GPa	σ_{sp} , GPa
1.020	73	8.15	4.09
0.952	56	17.33	3.13
3.995 [10]	44.3	27.5	2.48
3.999 [10]	52.5	27.5	2.93

σ_{max} is the maximum shock compressive stress.

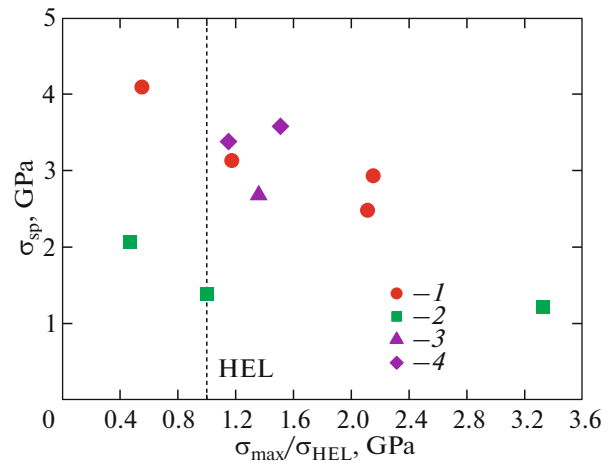


Fig. 4. The dependence of spall strength of tungsten carbide ceramics on the maximum compressive stress: (1) data obtained in this study and in [10] (at a maximum pressure); (2) data for hot-pressed WC, $\sigma_{HEL} = 7.2 \text{ GPa}$ [15]; (3) data for WC + 5.7% Co + 1.9% Ta [14]; (4) data for WC + 3–4% Ni + 0.4–0.8% Fe [14].

When the Hugoniot elastic limit is slightly exceeded, the spall strength value immediately drops to about 25% and decreases with a further increase in pressure.

The spall strength of hot-pressed tungsten carbide was studied in [15]. It was shown that an increase in the compressive stress in the shock wave from 3.4 to 7.2 GPa leads to a sharp decrease in the value of spall strength from 2.06 to 1.38 GPa, while a further increase in maximum compressive stress to 24 GPa slightly reduces this value to 1.22 GPa. Comparison of the results of the present study with the published data [15] shows a two-fold increase in spall strength of tungsten carbide ceramics synthesized by SPS in the comparable ranges of compressive stresses. The values of spall strength of tungsten carbide with $\sigma_{HEL} = 4.1 \text{ GPa}$ obtained in [14] with additions of 5.7% Co + 1.9% Ta and 3–4% Ni + 0.4–0.8% Fe are at the same level as the values for nonporous tungsten carbide (Fig. 4) at compressive stresses exceeding σ_{HEL} , which confirms the strengthening effect of additives.

CONCLUSIONS

An analysis of the measured free-surface velocity profiles of WC ceramics samples with a thickness from 0.15 to 4 mm synthesized by SPS shows strong decay of the elastic precursor wave during its propagation in the material. In the experiments with samples having a thickness of 0.5 mm or less, relaxation of stresses behind the front of the elastic precursor is clearly recorded. The measured values of the Hugoniot elastic limit and spall strength for the studied ceramics are more than twice higher than for hot-pressed ceramics [13, 15]. At maximum shock compressive stresses roughly twice exceeding the Hugoniot elastic limit of

the studied ceramics, a decrease in spall strength value by one third of its value in the elastic region is observed. The results of the experiments do not show signs of material destruction upon shock compression.

ACKNOWLEDGMENTS

This study was performed in accordance with State Assignment, topic no. 0089-2014-0016, and within the Program of Fundamental Studies of the Presidium of the Russian Academy of Sciences no. 13, “Condensed Matter and Plasma at High Energy Densities, Research Direction Quick Physicochemical Transformations and Fracture of Solid Bodies and Liquids.”

REFERENCES

1. D. E. Grady, *Mech. Mater.* **29**, 181 (1998). doi 10.1016/S0167-6636(98)00015-5
2. T. J. Ahrens and G. E. Duvall, *J. Geophys. Res.* **71**, 4349 (1966).
3. Z. Rosenberg, N. S. Brar, and S. J. Bless, *J. Phys. Colloq.* **49** (C3), 707 (1988). doi 10.1051/jphyscol:19883100
4. J. Cagnoux and F. Longy, *Proc. American Physical Society Topical Conf. “Shock Waves in Condensed Matter,” Monterey, United States, 1987* (Elsevier, Amsterdam, 1988), p. 293.
5. C. D. Adams, W. W. Anderson, W. R. Blumenthal, and G. T. Gray III, *J. Phys.: Conf. Ser.* **500**, 112001 (2014). doi 10.1088/1742-6596/500/11/112001
6. E. B. Zaretsky, *J. Appl. Phys.* **114**, 183518 (2013). doi 10.1063/1.4830014
7. I. Girelitsky, E. Zaretsky, S. Kalabukhov, M. P. Dariel, and N. Frage, *J. Appl. Phys.* **115**, 243505 (2014). doi 10.1063/1.4885436
8. A. S. Savinykh, G. I. Kanel, S. V. Razorenov, and V. I. Romyantsev, *Tech. Phys.* **58**, 973 (2013). doi 10.1134/S1063784213070207
9. O. Guillon, J. Gonzalez-Julian, B. Dargatz, T. Kessel, G. Schierring, J. Rathel, and M. Herrmann, *Adv. Eng. Mater.* **16**, 830 (2014). doi 10.1002/adem.201300409
10. A. S. Savinykh, K. Mandel, S. V. Razorenov, and L. Krueger, *Tech. Phys.* **63**, 357 (2018). doi 10.1134/S1063784218030210
11. G. I. Kanel, S. V. Razorenov, A. V. Utkin, and V. E. Fortov, *Shockwave Phenomena in Condensed Media* (Yanus-K, Moscow, 1996).
12. L. M. Bärker and R. E. Hollenbäch, *J. Appl. Phys.* **43**, 4669 (1972). <https://doi.org/10.1063/1.1660986>
13. D. P. Dandekar and D. E. Grady, *Proc. American Physical Society Conf. “Shock Compression of Condensed Matter,” Atlanta, United States, 2001*, Ed. by M. D. Furnish, N. N. Thadhani, and Y. Horie (American Inst. of Physics, 2002), pp. 783–786.
14. D. E. Grady, Report No. SAND94-3266 (Sandia National Laboratories, Albuquerque, 1995).
15. D. P. Dandekar, Report No. ARL-TR-3335 (US Army Research Laboratory, Aberdeen Proving Ground, 2004).

Translated by O. Kadkin